Intermetallics 18 (2010) 655–665

Contents lists available at ScienceDirect

Intermetallics

journal homepage: www.elsevier.com/locate/intermet

The Yb–Zn–Ga system: Partial isothermal section at 400 °C with 0–33.3 at.% Yb

Yu. Verbovytskyy*, A.P. Gonçalves

Departamento de Química, Instituto Tecnológico e Nuclear/CFMC–UL, Estrada Nacional 10, P—2686–953 Sacavém Codex, Portugal

ARTICLE INFO

Article history:
Received 1 July 2009
Received in revised form
29 October 2009
Accepted 4 November 2009
Available online 3 December 2009

Keywords:
A. Rare earth intermetallics
A. Ternary alloy systems
B. Phase diagrams
B. Phase identification

ABSTRACT

The phase relations in the ternary system Yb–Zn–Ga have been studied at 400 °C for the partial isothermal section in the 0–33.3 at.% ytterbium concentration range. X-ray powder diffraction (XRPD), optical microscopy (OM) and scanning electron microscopy (SEM), complemented with energy dispersive X-ray spectroscopy (EDS), were used to analyse the microstructures, identify the phases and characterize their crystal structures and compositions. The Yb–Zn–Ga partial section at 400 °C is characterized by the presence of an extended solid solution, $YbZn_{2-x}Ga_x$ ($0 \le x \le 1$), and the existence of four ternary intermetallic compounds, $YbZn_xGa_{4-x}$, $0.75 \le x \le 2$ ($BaAl_4$-type), $YbZn_xGa_{4-x}$, $0.25 \le x \le 0.5$ ($CaCu_{0.15}Ga_{3.85}$-type), $Yb_3Zn_{11-x}Ga_x$, $3.5 \le x \le 4.2$ (La_3Al_{11}-type) and $YbZn_{11-x}Ga_x$, $1.8 \le x \le 2.7$ ($BaHg_{11}$-type), the last three being reported here for the first time. Sixteen ternary phase fields have been identified in the studied partial isothermal section at 400 °C.

1. Introduction

Pure gallium metal and many gallium based alloys and intermetallic compounds have extensive technological applications and fundamental interest. Gallium arsenide (GaAs) and gallium nitride (GaN) are well known semiconductors. Gallium is used as a doping component in electronic devises (as in transistors or photovoltaic cells), for cold welding, with other metals (In, Sn) for producing low-melting alloys, etc. Moreover, unusual physical properties have been found in intermetallic gallides, as the unconventional superconductivity observed in $PuCoGa_5$. In order to develop new materials, there is an increasing interest for the investigation of the related gallium based alloys and intermetallic compounds.

The ternary (rare earth)-(*d*-metal) gallides have been extensively studied during the past decades. Two book reviews [1,2], containing information about the crystal structure of the ternary compounds and on some R–M–Ga phase diagrams, have been published 20 years ago. A more deep analysis on the interaction among the components in the Ga-based ternary systems has been done in a recent work [3]. The systematic oriented investigations were mainly performed on the R–{Mn, Fe, Co, Ni, Cu}–Ga systems, and only some specific compositions were studied in the remaining systems [4]. However, the interest on the crystal structure and physical properties of other systems, as the ytterbium–(transition metal)–gallium ones, is increasing due to their interesting physical properties, such as heavy fermion behaviour, spin fluctuations and mixed valence.

In the present paper we report for the first time a study on the partial isothermal section of the Yb–Zn–Ga system at 400 °C, with 0–33.3 at.% Yb, together with the crystal structure identification of the new ternary phases stable at this temperature.

2. Literature data

A brief summary of the literature data focusing on the phase equilibria of the binary Yb–Zn–Ga subsystems is presented below. A list of the solid phases formed in the three binary systems involved is given in Table 1.

The Yb–Zn phase diagram has been established by Mason and Chiotti [5]. Six binary compounds exist in this system: YbZn (CsCl-type), $YbZn_2$ ($CeCu_2$-type), Yb_3Zn_{11} (La_3Al_{11}-type), $Yb_{13}Zn_{58}$ ($Gd_{13}Zn_{58}$-type), Yb_2Zn_{17} (Th_2Zn_{17}-type) and $YbZn_{11}$ ($BaCd_{11}$-type). Five of them, YbZn, $YbZn_2$, $Yb_{13}Zn_{58}$, Yb_2Zn_{17} and $YbZn_{11}$ melt congruently at 650, 751, 752, 754 and 755 °C, respectively. The Yb_3Zn_{11} is obtained by the peritectic reaction $L + Yb_{13}Zn_{58} = Yb_3Zn_{11}$ at 695 °C. The $YbZn_2$ and Yb_2Zn_{17}, according to [5] and [6], have two polymorphic modifications (unknown-type and Th_2Ni_{17}-type, respectively). Also, authors [6] pointed out on existence of the Yb_3Zn_{17} (Ru_3Be_{17}-type) and $YbZn_{13}$ ($NaZn_{13}$-type) intermetallics.

The first versions of the Yb–Ga phase diagram, in the whole concentration range, were reported in [7] and [8]. Latter, contributions to the Yb–Ga system, mainly in the Ga-rich corner, were made in papers [9,10]. A generalized Yb–Ga phase diagram, based

* Corresponding author. Departamento de Química, Instituto Tecnológico e Nuclear/CFMC–UL, Estrada Nacional 10, P—2686–953 Sacavém Codex, Portugal. Tel.: +351 219946100; fax: +351 219946185.
E-mail address: yuryvv@bigmir.net (Yu. Verbovytskyy).

0966-9795/$ – see front matter © 2009 Elsevier Ltd. All rights reserved.
doi:10.1016/j.intermet.2009.11.001

Table 1
Literature data on binary and ternary phases of the Yb–Zn–Ga system.

Phase	Transformation Temperature (°C)[a]	Structure type	Space group	Lattice parameters (Å)			Reference
				a	*b*	*c*	
YbZn	650, mp	CsCl	$Pm\bar{3}m$	3.629	–	–	[5]
$YbZn_2$ (α)	751, mp	–	–	–	–	–	[5]
$YbZn_2$ (β)	630, pc	$CeCu_2$	Imma	4.570	7.290	7.562	[5]
Yb_3Zn_{11}	695, p	La_3Al_{11}	Immm	4.421	8.891	13.127	[5]
$Yb_{13}Zn_{58}$	752, mp	$Gd_{13}Zn_{58}$	$P6_3mc$	14.32	–	14.15	[6]
Yb_3Zn_{17}	?	Ru_3Be_{17}	$Im\bar{3}$	14.291	–	–	[6]
Yb_2Zn_{17} (α)	754, mp	Th_2Ni_{17}	$P6_3/mmc$	9.022	–	8.798	[4]
Yb_2Zn_{17} (β)	?	Th_2Zn_{17}	$R\bar{3}m$	9.040	–	13.216	[5]
$YbZn_{11}$	755, mp	$BaCd_{11}$	$I4_1/amd$	10.637	–	6.822	[5]
$YbZn_{13}$	?	$NaZn_{13}$	$Fm\bar{3}c$	12.172	–	–	[4]
$YbGa_6$	282, p	$PuGa_6$	P4/nbm	5.849	–	7.601	[12]
$YbGa_5$	333, p	$YbGa_5$	I4/mmm	4.3059	–	25.871	[10]
$YbGa_4$	755, p	$CaGa_4$	C2/m	6.148 $\beta = 118.86°$	6.106	6.084	[9]
$YbGa_{3-x}$ $(0 \le x \le 0.36)$	735, pr	$YbGa_{2.64}$	P6/mmm	13.025	–	8.360	[9]
Yb_3Ga_8	868, p	Eu_3Ga_8	Immm	4.225	4.340	25.665	[9]
$YbGa_2$	1100, mp	$CaIn_2$	$P6_3/mmm$	4.456	–	7.187	[13]
YbGa	895, mp	TiCu	P4/mmm	3.42	–	3.94	[7]
Yb_2Ga	650, p	Co_2Si	Pnma	7.063	5.050	9.427	[7]
$YbZn_xGa_{4-x}$ $(0.25 \le x \le 1)$	?	$BaAl_4$	I4/mmm	4.2428–4.2021		10.968–10.955	[16]

[a] mp = melting point, p = peritectic reaction; pc = polymorphic reaction; pr = peritectoid reaction.

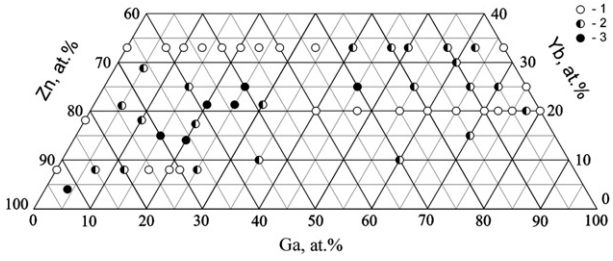

Fig. 1. Compositions of the Yb–Zn–Ga samples quenched from 400 °C (1 – single-phase, 2 – two-phase, 3 – three-phase samples).

on experimental data and thermodynamic calculations, is presented in paper [11]. The existence of nine compounds has been established: $YbGa_6$ ($PuGa_6$-type), $YbGa_5$ ($YbGa_5$-type), $YbGa_4$ ($CaGa_4$-type), $YbGa_{3-x}$ ($YbGa_{2.64}$-type), Yb_3Ga_8 (Eu_3Ga_8-type), $YbGa_2$ ($CaIn_2$-type), YbGa (TiCu-type) and Yb_2Ga (Co_2Si-type) [7–13]. Four compounds, $YbGa_6$, $YbGa_5$, $YbGa_4$ and Yb_3Ga_8, are formed peritectically at 282, 333, 755 and 868 °C, respectively. The binary, $YbGa_2$, YbGa and Yb_2Ga, compounds melt congruently at 1100, 895 and 655 °C, respectively. Additionally, the $YbGa_{3-x}$ intermetallics are formed by a peritectoid reaction and are stable below 735 °C.

Experimental investigations and thermodynamic studies of the Zn–Ga phase diagram have been reported in papers [14,15]. There

Table 2
New ternary phases in the Yb–Zn–Ga systems.

Phase	Structure type	Space group	Lattice parameters (Å, Å^3)				Remark
			a	*b*	*c*	*V*	
$Yb_{13}Zn_{58-x}Ga_x$ $(0 \le x \le 7)$	$Gd_{13}Zn_{58}$	$P6_3/mmc$	14.317(2)	–	14.173(3)	2515.9(8)	$x = 0$[a]
			14.348(2)	–	14.095(2)	2512.9(5)	$x = 7$[a]
$YbZn_{2-x}Ga_x$ $(0 \le x \le 1)$	$CeCu_2$	Imma	4.5668(8)	7.2866(11)	7.5643(12)	251.71(7)	$x = 0$[a]
			4.4803(5)	7.2281(7)	7.6440(8)	247.54(4)	$x = 1$[a]
			4.4838(3)	7.2084(4)	7.6622(5)	247.65(3)	$x = 1$[b]
$YbZn_xGa_{4-x}$ $(0.25 \le x \le 0.5)$ (τ_1)	$CaCu_{0.15}Ga_{3.85}$	C2/m	11.4747(3)	4.2381(1) $\beta = 110.642(1)°$	4.3445(1)	197.71(1)	$x = 0.25$[b]
			11.5091(7)	4.2070(2) $\beta = 110.564(3)°$	4.3405(2)	196.77(2)	$x = 0.36$[b]
			11.5409(2)	4.2007(1) $\beta = 110.592(1)°$	4.3236(1)	196.21(1)	$x = 0.5$[b]
$YbZn_xGa_{4-x}$ $(0.75 \le x \le 2)$ (τ_2)	$BaAl_4$	I4/mmm	4.2141(1)	–	10.9182(3)	193.91(1)	$x = 0.75$[b]
			4.1904(1)	–	10.9718(3)	192.66(1)	$x = 1$[b]
			4.1802(1)	–	10.9901(2)	192.04(1)	$x = 1.25$[b]
			4.1678(1)	–	10.9994(2)	191.07(1)	$x = 1.6$[b]
			4.1761(1)	–	10.9213(2)	190.46(1)	$x = 2$[b]
$Yb_3Zn_{11-x}Ga_x$ $(3.5 \le x \le 4.2)$ (τ_3)	La_3Al_{11}	Immm	4.3150(1)	9.4482(3)	12.7121(4)	518.26(3)	$x \sim 3.5$[b]
			4.3109(1)	9.4763(3)	12.7016(4)	518.89(3)	$x \sim 4.2$[b]
$YbZn_{11-x}Ga_x$ $(1.8 \le x \le 2.7)$ (τ_4)	$BaHg_{11}$	$Pm\bar{3}m$	8.4164(1)	–	–	596.18(1)	$x = 2$[b]
			8.4288(1)	–	–	598.82(1)	$x = 2.4$[b]
			8.4360(1)	–	–	600.35(1)	$x = 2.7$[b]

[a] As-prepared sample.
[b] Annealed sample.

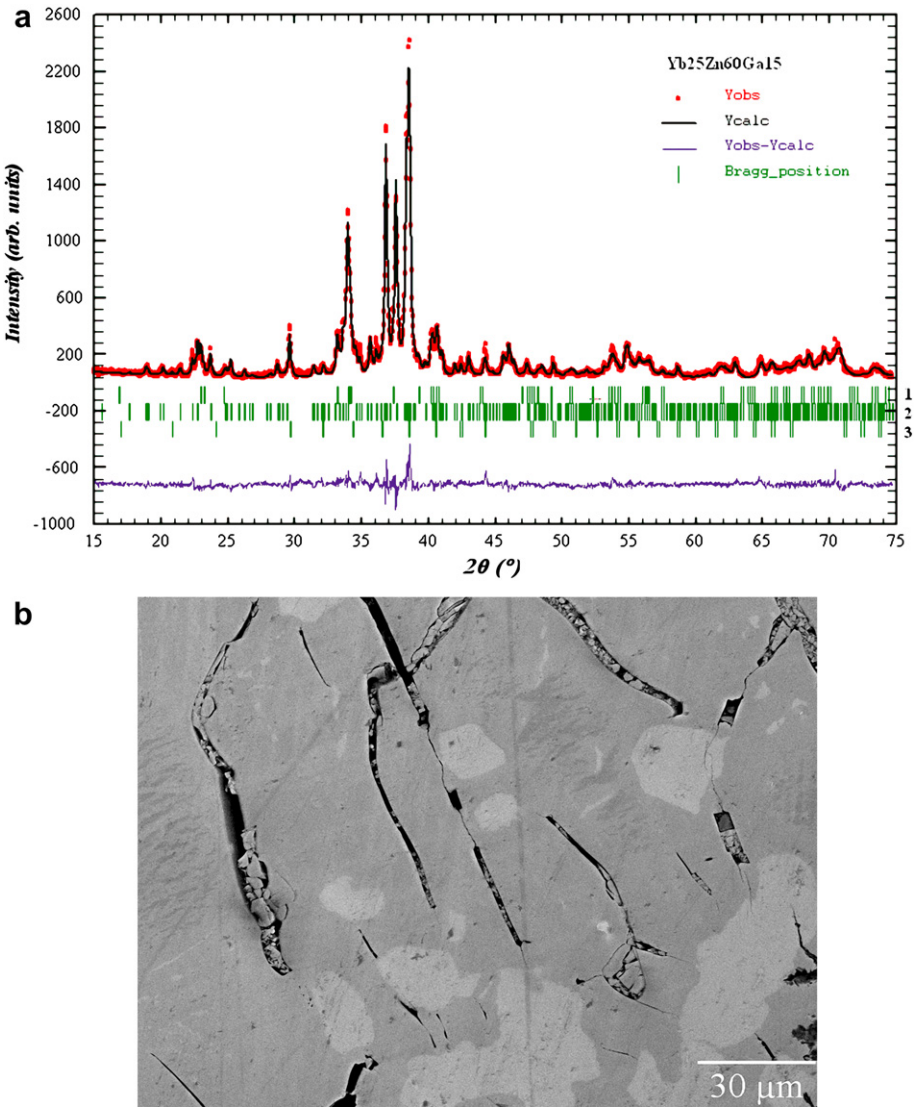

Fig. 2. X-ray diffraction pattern (a) and microstructure (b) of the annealed $Yb_{25}Zn_{60}Ga_{15}$ alloy (1 – $YbZn_{2-x}Ga_x$ (white phase), 2 – $Yb_{13}Zn_{58-x}Ga_x$ (dark phase), 3 – Yb_2O_3).

are no binary compounds in all the Zn–Ga system. Only one eutectic reaction, with the ~3.7Zn:96.3Ga composition, is observed in this system at 25 °C.

Up to the author's best knowledge, there is no data in the literature on the interaction of the components in the Yb–Zn–Ga system. Only one compound, $YbZn_xGa_{4-x}$ ($0.25 \leq x \leq 1$), reported to crystallize in the $BaAl_4$ structure type [16], has been described up to now on this system. No information on the forming characteristics of this compound was given.

3. Experimental details

A total of fifty four binary and ternary samples have been prepared and analysed in the present work, their compositions being shown in Figure 1. Metals with nominal purities >99.95 wt.% (ytterbium ingots, zinc tear drops and gallium pieces) were used as starting materials. Each sample was synthesized by directly melting the elements inside quartz ampoules under vacuum (10^{-5} Torr). The reactions were first performed at 900 °C, the ampoules being hold at that temperature for one hour, followed by their cooling to 400–500 °C in air and further under running water. The obtained products, with metallic-like lustres, were studied by X-ray powder diffraction technique. No reaction with the quartz ampoules was observed. Finally, fragments of the as-prepared ingots were sealed in evacuated quartz tubes and annealed at 400 °C for 20 days, inside a vertical oven. After the heat treatments, the samples were quenched by submerging the quartz tubes in cold water and analysed.

A PANalytical X'Pert Pro diffractometer (CuK_α-radiation) was used for the X-ray phase and structural analyses of the powdered polycrystalline samples. The scans were taken in the $\theta/2\theta$ mode with the following parameters: 2θ region, 15–120°; step scan, 0.03°; counting time per step, 2–20 s. The theoretical powder patterns were calculated with the help of the PowderCell program [17] and used for the identification of the phases. The lattice parameters were obtained by least-squares fitting using the Latcon program [18]. The FullProf [19] program was used for single and multi phase Rietveld fittings.

The microstructure of the samples was first studied, on polished and etched surfaces, by using an optical microscope Olympus OM150. Selected samples were then observed by electron microscopy, by using a Hitachi S2400 scanning electron microscope

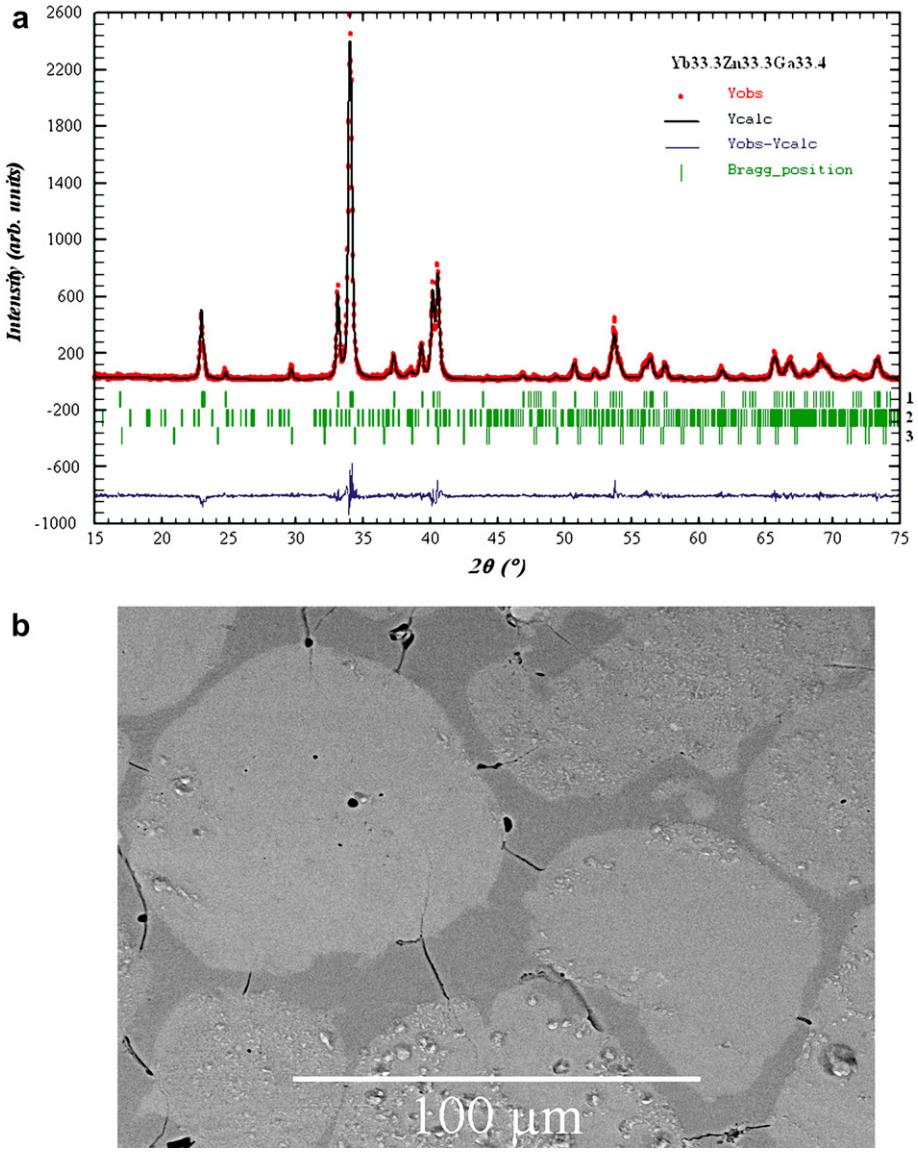

Fig. 3. X-ray diffraction pattern (a) and microstructure (b) of the annealed $Yb_{33.3}Zn_{33.3}Ga_{33.4}$ alloy (1 – YbZnGa (grey grains), 2 – $Yb_{13}Zn_{58-x}Ga_x$ (dark phase), 3 – Yb_2O_3).

Table 3
Crystallographic data and details of experimental conditions and structure refinement for the YbZnGa phase.

Empirical formula	YbZnGa
Structure type	$CeCu_2$ (KHg_2)
Crystal system	Orthorhombic
Space group	*Imma*
Pearson symbol, Z	*tI*12, 4
Diffractometer	PANalytical X'Pert Pro (CuK_α-radiation)
2θ range, step (°), counting time (s)	15–120, 0.03, 15
Unit cell parameters	See Table 2
Reliability factors	
R_B, R_F	3.82, 2.18
R_p, R_{wp}	7.72, 10.4
Atom position	
Yb in 4*e* (0, ¼, *z*), B_{iso} (Å^2)	$z = 0.5401(3)$, 1.49(5)
M in 8*h* (0, *y*, *z*), B_{iso} (Å^2)	$y = 0.0470(3)$, $z = 0.1647(3)$, 1.65(3)
Composition of M	0.5Zn + 0.5Ga

operated at 25 kV. The phases were analysed by semi-quantitative energy dispersive X-ray spectroscopy (EDS) using a Röntec detector with a protective beryllium window. At least three valid EDS point analyses were made for each phase in order to guarantee a good analysis of their compositions. These analyses were carried out with a spatial resolution of ~2 μm and a collection time of 100 s. Automated matrix corrections were carried out using the Röntec Edwin EDS software package.

4. Results and discussion

Samples from the gallium-rich region usually contain the binary $YbGa_4$, $YbGa_{3-x}$ and $YbGa_2$ compounds, in agreement with the literature data, which indicate that they are stable at 400 °C. The existence of other five binary phases from the Yb–Zn system ($YbZn_{11}$, Yb_2Zn_{17}, $Yb_{13}Zn_{58}$, Yb_3Zn_{11} and $YbZn_2$), also previously reported to be stable at that temperature, was confirmed, their crystallographic analysis agreeing with the reported data. The two previously described $YbZn_{13}$ and Yb_3Zn_{17} compounds were not

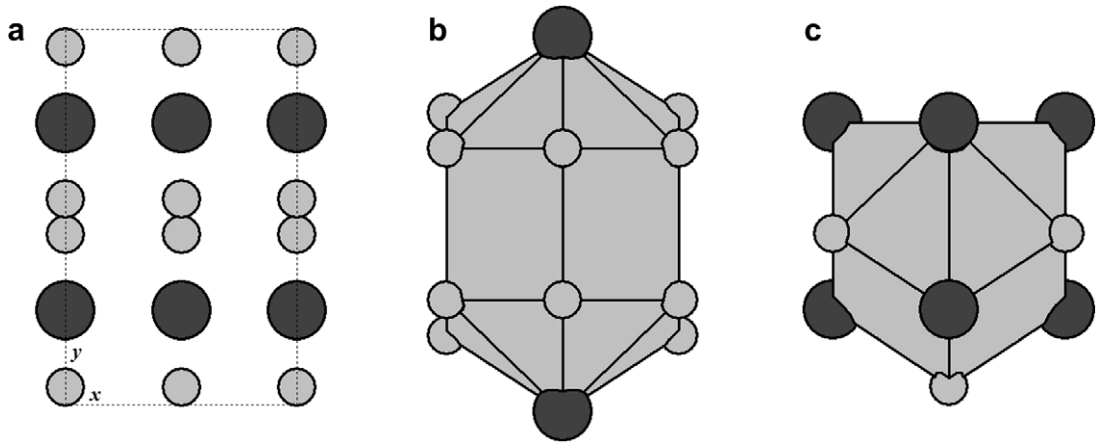

Fig. 4. Unit cell (a) and coordination polyhedral for Yb (b) and M (Zn and Ga) (c) atoms in the structure of YbZnGa. Dark circles indicate Yb atoms, while M (Zn and Ga) atoms are represented by light circles.

detected in the present work. This, together with their absence in the published binary Yb–Zn phase diagram, clearly points to a metastable nature of $YbZn_{13}$ and Yb_3Zn_{17}. Most probably, they are stabilized by small amounts of impurities or by kinetic reasons, which still needs further investigations.

After the annealing procedure, the binary $YbZn_{11}$, Yb_2Zn_{17} and Yb_3Zn_{11} compounds were found to dissolve only a small quantity of gallium (less than 5 at.%). The solubility of gallium in the binary $Yb_{13}Zn_{58}$ compound is ~7 at.% in annealed samples and up to ~10 at.% in as-prepared alloys. Lattice parameters for the as-prepared $Yb_{13}Zn_{58}$ and $Yb_{13}Zn_{51}Ga_7$ alloys are presented in Table 2.

An extended homogeneity range based on the binary $YbZn_2$ compound, along the $YbZn_2$–$YbGa_2$ section, was found, dissolving gallium up to the YbZnGa composition. The X-ray diffraction pattern and microstructure of the $Yb_{25}Zn_{60}Ga_{15}$ alloy, respectively, are plotted in Fig. 2a and b. A two-phase mixture can be observed, formed by YbZnGa (white region, $CeCu_2$-type) and $Yb_{13}Zn_{58-x}Ga_x$ (dark region, $Gd_{13}Zn_{58}$-type). Fig. 3a and b shows, respectively, the X-ray diffraction pattern and microstructure of the $Yb_{33.3}Zn_{33.3}Ga_{33.4}$ alloy. According to the XRD data, the sample consists of two phases: YbZnGa (main phase, $CeCu_2$-type) and $Yb_{13}Zn_{58-x}Ga_x$ (secondary phase, $Gd_{13}Zn_{58}$-type). Lattice parameters of YbZnGa are shown in Table 2. The microstructural analysis of the annealed sample confirms the XRD data: SEM/EDS studies indicate that the composition of the grey grains is closed to the Yb:Zn:Ga, while the composition of intergranular dark phase is consistent with the $Yb_{13}Zn_{58-x}Ga_x$ compound. White dots on surface of sample correspond to ytterbium oxides.

The Rietveld crystal structure refinement of the $YbZn_{2-x}Ga_x$ solid solution has been performed for the YbZnGa nominal composition sample, the results of being presented in Table 3. Herein, the Yb atoms occupy the position of the Ce atoms, and a statistical mixture of the Zn and Ga atoms fills the Cu atoms position in the $CeCu_2$ structure type. Projection of the YbZnGa structure on XY plate and coordination polyhedra for the different atoms are shown in Fig. 4. Coordination polyhedra for Yb atoms are distorted two-capped hexagonal prisms (coordination number 14). The M (Zn and Ga) atoms are inside of 10-vertex polyhedra. Interatomic distances for the YbZnGa are presented in Table 4. These distances are close to the sum of the atomic radii of the respective atoms. The shortest Yb–Yb, Yb–M and M–M bonds are equal 3.659(1), 3.103(2) and 2.592(2) Å, respectively.

A non-existing, or negligible, zinc solubility in the binary $YbGa_4$ and $YbGa_2$ compounds can be deduced from the X-ray phase analysis.

In the as-prepared and annealed alloys with compositions along the cross-section with 20 at.% ytterbium and a small amount of zinc a new ternary compound (τ_1) was found. This new intermetallic phase has a small homogeneity range, which extends from $YbZn_{0.25}Ga_{3.75}$ to $YbZn_{0.5}Ga_{3.5}$, and crystallizes with $CaCu_{0.15}Ga_{3.85}$ structure type (space group C2/m) [20]. X-ray diffraction pattern of the as-prepared $Yb_{20}Zn_{7.5}Ga_{72.5}$ alloy is presented in Fig. 5a. The cell parameters obtained during the XRD data fitting of annealed $YbZn_xGa_{4-x}$ ($0.25 \leq x \leq 0.5$) samples are shown in Table 2.

The early reported ternary $YbZn_xGa_{4-x}$ compound [16], with $BaAl_4$ structure type (space group I4/mmm) [21], was confirmed to be stable at 400 °C. According to our investigations, a homogeneity range of the above mentioned compound (τ_2), in annealed and as-prepared $YbZn_xGa_{4-x}$ alloys, was established with x from ~0.75 to ~2. Calculated lattice parameters of this intermetallic compound are presented in Table 2. X-ray diffraction pattern of as-prepared $Yb_{20}Zn_{15}Ga_{65}$ alloy is presented in Fig. 5b.

Fig. 6a and b shows the X-ray diffraction pattern and microstructure of the $Yb_{25}Zn_{30}Ga_{45}$ alloy, respectively. According to the XRD data, this alloy consists of three phases: $YbGa_2$ ($CaIn_2$-type), ~YbZnGa (CeCu-type) and ~$YbZn_2Ga_2$ ($BaAl_4$-type). Microprobe analyses of the $Yb_{25}Zn_{30}Ga_{45}$ sample agree with the XRD results, revealing the formation of the $YbZn_xGa_{4-x}$ compound (grey main phase), with ~$Yb_{20}Zn_{36}Ga_{44}$ average composition, together with big grains consisting of two phases (bright and dark dots), which correspond to the $YbGa_2$ and YbZnGa intermetallics (according to the XRD data).

The X-ray diffraction pattern and microstructure of the $Yb_{15}Zn_{70}Ga_{15}$ alloy, respectively, are displayed in Fig. 7a and b. X-ray

Table 4
Interatomic distances (d) and coordination number (CN) of the atoms in the structure of YbZnGa

Atoms		d (Å)	CN	Atoms		d (Å)	CN
Yb	–4M	3.103(2)	14	M	–2M	2.592(2)	10
	–2M	3.114(3)			–M	2.613(3)	
	–2M	3.227(3)			–M	2.927(3)	
	–4M	3.244(2)			–2Yb	3.103(2)	
	–2Yb	3.656(1)			–Yb	3.114(3)	
					–Yb	3.227(3)	
					–2Yb	3.244(2)	

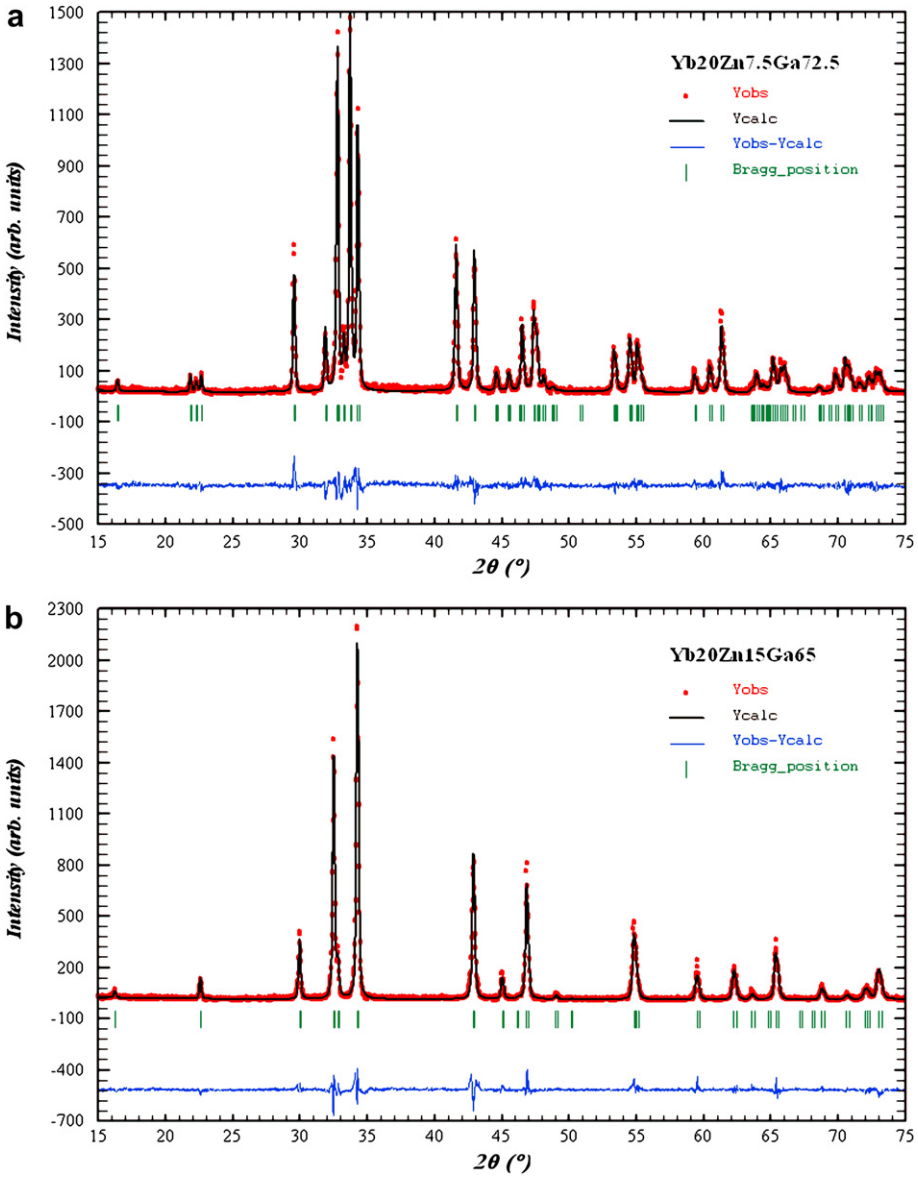

Fig. 5. X-ray diffraction pattern of as-prepared $Yb_{20}Zn_{7.5}Ga_{72.5}$ (a) and $Yb_{20}Zn_{15}Ga_{65}$ (b) alloys.

phase analysis of the above cited alloy indicated the existence of three phases: the major $YbZn_2Ga_2$ ($BaAl_4$-type) and $YbZn_{11}$ ($BaCd_{11}$-type), and minor amounts of Yb_2Zn_{17} (Th_2Zn_{17}-type). This result is in good agreement with the microprobe analyses. According to the SEM/EDS studies, this sample is mainly formed by a bright and grey phases, which correspond to the $YbZn_2Ga_2$ ($\sim Yb_{20}Zn_{42}Ga_{38}$) and $YbZn_{11}$ ($\sim Yb_8Zn_{89}Ga_3$) intermetallic compounds, respectively. The XRD pattern and microstructure of the $Yb_{17}Zn_{63}Ga_{20}$ alloy are shown in Fig. 8a and b, respectively. Based on XRD data as well as on SEM/EDS studies it can be concluded that this alloy consists of only two phases: the ternary $YbZn_2Ga_2$ (bright phase) and binary Yb_2Zn_{17} (grey phase) compounds.

X-ray phase analysis of some as-cast samples, whose composition lies along the 21.5 at.% ytterbium concentration and has 20–30 at.% gallium, shown the existence of a new ternary $Yb_3Zn_{11-x}Ga_x$ (τ_3) compound with small homogeneity range ($x \sim 3.5$–4.2). This intermetallic compound crystallizes with the La_3Al_{11} structure type. Calculated lattice parameters for $\sim Yb_3Zn_{7.5}Ga_{3.5}$ and $\sim Yb_3Zn_{6.8}Ga_{4.2}$, which were obtained from an almost single-phase sample, are shown in Table 2. The X-ray diffraction pattern of the phase sample with the composition $Yb_{21.5}Zn_{53.5}Ga_{25}$ is presented in Fig. 9. Annealed alloys with 21.5 at.% Yb and small amounts of Ga fall into three-phase or two-phase regions, which consist of $Yb_{13}Zn_{58-x}Ga_x$, $YbZn_{2-x}Ga_x$ and Yb_3Zn_{11} compounds.

In the as-prepared as well as in the annealed at 400 °C samples in Zn-rich corner we found a new intermetallic compound, $YbZn_{11-x}Ga_x$ ($1.8 \leq x \leq 2.7$) (τ_4), with a small homogeneity range, which crystallizes with the $BaHg_{11}$ structure type (space group $Pm\bar{3}m$) [21]. Calculated lattice parameters for this phase are shown in Table 2. The X-ray diffraction pattern of an annealed $Yb_8Zn_{79}Ga_{13}$ alloy is presented in Fig. 10a. It consists of three phases: $YbZn_{11-x}Ga_x$ ($BaHg_{11}$-type, main phase), $YbZn_{11}$ ($BaCd_{11}$-type) and Zn (Mg-type). The X-ray diffraction pattern of the $Yb_{8.3}Zn_{75.5}Ga_{16.2}$ nominal composition alloy points to a single-phase sample, as can be see in Fig. 10b.

The crystallographic data on the new ternary Yb–Zn–Ga phases are collected in Table 2. Herein, we present only the lattice parameters of these compounds. Single crystal studies, accurate crystal structure determination, magnetic and transport physical

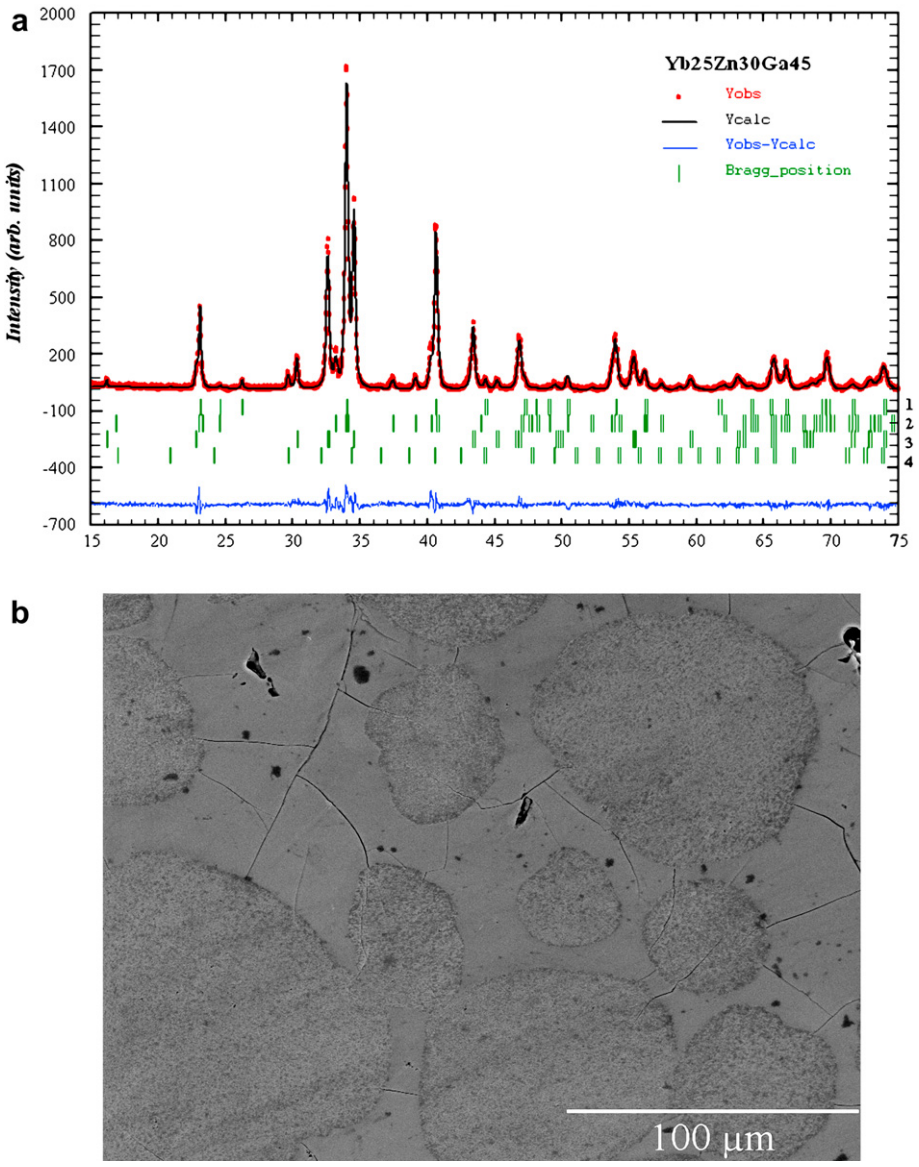

Fig. 6. X-ray diffraction pattern (a) and microstructure (b) of the annealed $Yb_{25}Zn_{30}Ga_{45}$ alloy (1 – $YbGa_2$ (grains), 2 – YbZnGa (grains), 3 – $YbZn_2Ga_2$ (dark phase), 4 – Yb_2O_3).

properties of ternary Yb–Zn–Ga phases will publish in a further paper.

The isothermal section at 400 °C of the Yb–Zn–Ga phase diagram (0–33.3 at.% Yb), constructed by using the experimental results obtained from the X-ray powder diffraction experiments and SEM/EDX analysis, is shown in Fig. 11. In this partial isothermal section sixteen ternary phase fields have been identified, those are listed below in order of increasing of zinc contents:

1) $L + YbGa_4 + YbZn_xGa_{4-x}$ (τ_1),
2) $L + YbZn_xGa_{4-x}$ (τ_1) + $YbZn_xGa_{4-x}$ (τ_2),
3) $YbGa_4 + YbZn_xGa_{4-x}$ (τ_1) + $YbGa_{3-x}$,
4) $YbZn_xGa_{4-x}$ (τ_1) + $YbGa_{3-x} + YbGa_2$,
5) $YbZn_xGa_{4-x}$ (τ_1) + $YbZn_xGa_{4-x}$ (τ_2) + $YbGa_2$,
6) $YbZn_xGa_{4-x}$ (τ_2) + $YbGa_2 + YbZn_{2-x}Ga_x$,
7) $YbZn_xGa_{4-x}$ (τ_2) + $YbZn_{11-x}Ga_x$ (τ_4) + L,
8) $YbZn_xGa_{4-x}$ (τ_2) + $YbZn_{11-x}Ga_x$ (τ_4) + $YbZn_{11}$,
9) $YbZn_xGa_{4-x}$ (τ_2) + $YbZn_{11} + Yb_2Zn_{17}$,
10) $YbZn_xGa_{4-x}$ (τ_2) + $Yb_3Zn_{11-x}Ga_x$ (τ_3) + Yb_2Zn_{17},
11) $YbZn_xGa_{4-x}$ (τ_2) + $YbZn_{2-x}Ga_x + Yb_3Zn_{11-x}Ga_x$ (τ_3),
12) $YbZn_{2-x}Ga_x + Yb_3Zn_{11-x}Ga_x$ (τ_3) + $Yb_{13}Zn_{58-x}Ga_x$,
13) $Yb_3Zn_{11-x}Ga_x$ (τ_3) + $Yb_{13}Zn_{58-x}Ga_x + Yb_2Zn_{17}$,
14) $YbZn_{11-x}Ga_x$ (τ_4) + L + Zn,
15) $YbZn_{11-x}Ga_x$ (τ_4) + Zn + $YbZn_{11}$,
16) $YbZn_{2-x}Ga_x + Yb_{13}Zn_{58-x}Ga_x + Yb_3Zn_{11}$.

Table 5 shows a comparison on interaction with ytterbium, *d*-transition and gallium metals. Among the 30 possible Yb–M–Ga (M = *d*-metal) systems, the isothermal sections were investigated, in the partial or whole concentration region, only for the nine systems, and 95 ternary compounds were found [1–4]. The rare earth gallium systems with *d*-element from the IB and VIIIA periodic groups are usually rich in the number of ternary compounds. Up to now, all the known ternary gallides with established crystal structures were identified in the 0–40 at.% ytterbium region. They exist with a variety compositions and structure types: Mo_2NiB_2, $MgZn_2$, $CeCu_2$, TiNiSi, Mg_2Cu_3Si, $CaCu_5$, $PrFe_7$, $ThMn_{12}$, $ScFe_6Ga_6$, Th_2Zn_{17}, Na_3As, $NaZn_{13}$, $BaHg_{11}$, $AuBe_5$,

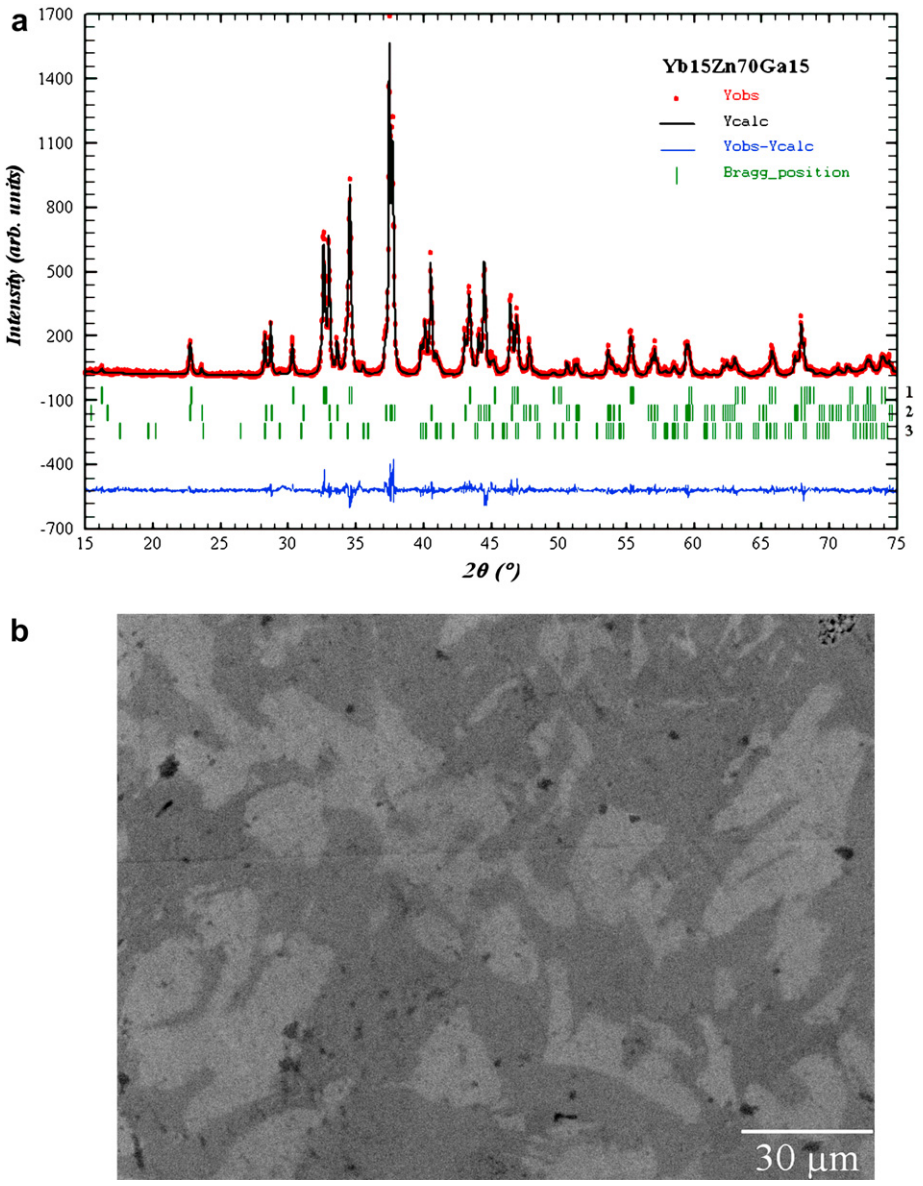

Fig. 7. X-ray diffraction pattern (a) and microstructure (b) of the annealed $Yb_{15}Zn_{70}Ga_{15}$ alloy (1 – $YbZn_2Ga_2$ (bright phase), 2 – $YbZn_{11}$ (grey phase), 3 – Yb_2Zn_{17}).

YCd_6, $Cd_{14}Ag_{51}$, $YbAg_{3.1}Ga_{2.6}$ $YbAg_{3.6}Ga_{1.9}$, $YbAg_{2.5}Ga_{2.1}$, $YbAu_{4.2}Ga_{1.8}$, $BaAl_4$, $CaCu_{0.15}Ga_{3.85}$, La_3Al_{11}, $Yb_3Au_{5.5}Ga_{5.5}$, $CeNi_3$, $DyCo_{6.6}Ga_{1.9}$, $Sm_{15}Ni_{52}Ga_{44}$, $HoNi_{2.6}Ga_{2.4}$, $Ce_3Ni_6Si_2$, $MgCuAl_2$, $CeNiSi_2$, $YbAgGa_2$, Lu_2CoGa_3, $Ce_{2-x}Pt_4Ga_{8+y}$, $Ho_4Ni_{10}Ga_{21}$, $Y_2Co_3Ga_9$, $TmNi_3Ga_7$, $ScRh_3Si_7$, $YNiAl_4$, $Yb_2Ru_3Ga_{10}$, $ErNi_3Al_9$, Y_4PdGa_{12}, $HoCoGa_5$, Ho_2CoGa_8, $CeFe_2Al_8$ [1–4].

The formation of solid solutions, with extended homogeneity ranges, based on some binary compounds and ternary phases is also common in the Yb–M–Ga systems. For example, a wide $YbM_{2-x}Ga_x$ solid solution based on the binary $YbAg_2$ compound, crystallizing with the $CeCu_2$-type structure, has been reported in [22], its limit composition being $YbAg_{0.2}Ga_{1.8}$. Up to the our best knowledge, transformation of the structures along the "row" $CaGa_4$ ($YbGa_4$)–$CaCu_{0.15}Ga_{3.85}$ (YbM_xGa_{4-x})–$BaAl_4$ (YbM_xGa_{4-x})–La_3Al_{11} ($Yb_3M_{11-x}Ga_x$) has been established in the Yb–M–Ga systems with M = Cu, Ag, Au, Pd, Pt [3] and Zn. The relationship among the above mentioned structures is schematically presented in Fig. 12. The $CaGa_4$ and $CaCu_{0.15}Ga_{3.85}$ are distorted variants of the $BaAl_4$ structure type. The La_3Al_{11} structure can be obtained from $BaAl_4$ by considering three unit cells and merging part of the 4*e* positions from this last structure type into the 2*d* positions of the La_3Al_{11} structure. Therefore, the difference between the $BaAl_4$ and La_3Al_{11} compositions is a result of this merging. Albeit the large number of systems having compounds with the four above mention structure types, ternary gallides with $BaHg_{11}$ structure type have been found only in two of them, Yb–Pd–Ga [3] and Yb–Zn–Ga.

5. Conclusion

Fifty four binary and ternary samples belonging to the Yb–Zn–Ga system have been analysed by means of optical and electron microscopy, powder X-ray diffraction and EDS measurements. The existence of the seven compounds from the binary Yb–Ga and Yb–Zn systems reported to be stable at 400 °C has been confirmed during the study of the partial isothermal section of the Yb–Zn–Ga phase diagram at that temperature. The interaction of the components in this system leads to the formation of four ternary compounds (three of them reported here for the first time):

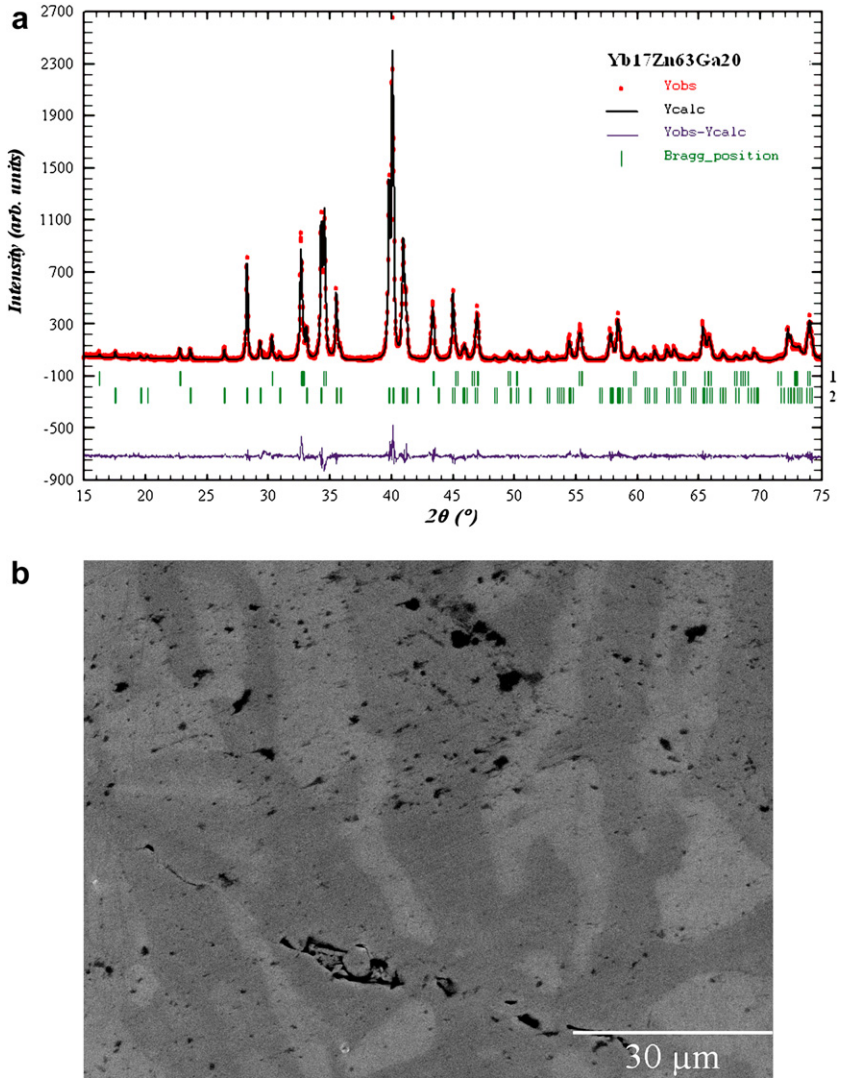

Fig. 8. X-ray diffraction pattern (a) and microstructure (b) of the annealed $Yb_{17}Zn_{63}Ga_{20}$ alloy (1 – $YbZn_2Ga_2$ (bright phase), 2 – Yb_2Zn_{17} (grey phase)).

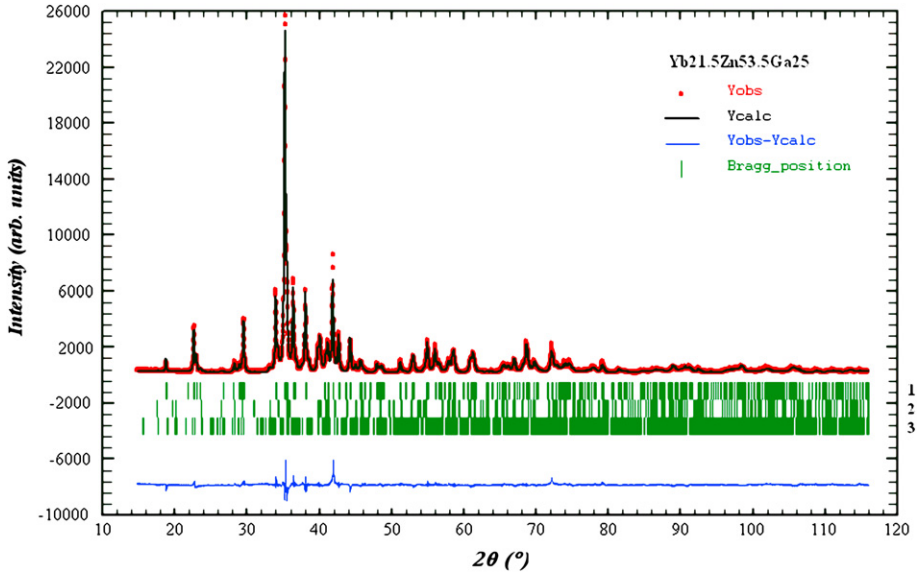

Fig. 9. X-ray diffraction pattern of annealed $Yb_{21.5}Zn_{53.5}Ga_{25}$ alloy (1 – $Yb_3Zn_{11-x}Ga_x$, 2 – Yb_2Zn_{17}, 3 – $Yb_{13}Zn_{58-x}Ga_x$).

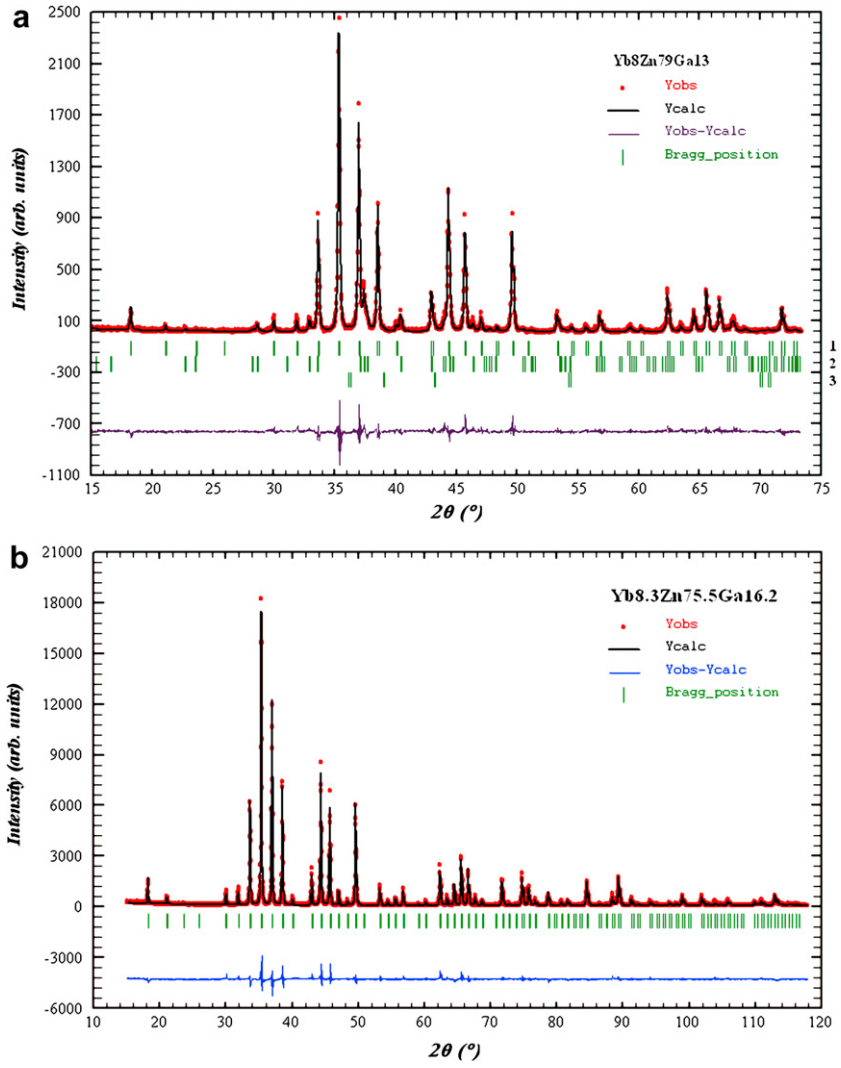

Fig. 10. X-ray diffraction pattern of annealed $Yb_8Zn_{79}Ga_{13}$ (*a*) and $Yb_{8.3}Zn_{75.5}Ga_{16.2}$ (*b*) alloys (1 – $YbZn_{11-x}Ga_x$, 2 – $YbZn_{11}$, 3 – Zn).

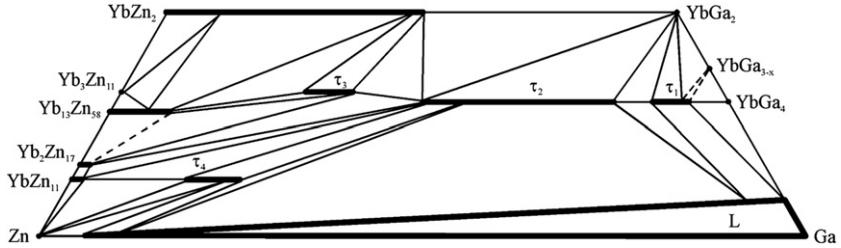

Fig. 11. Isothermal section of the ternary Yb–Zn–Ga phase diagram at 400 °C with 0–33.3 at.% Yb. τ_1 – $YbZn_{0.25-0.5}Ga_{3.75-3.5}$; τ_2 – $YbZn_{0.75-2}Ga_{3.25-2}$; τ_3 – $Yb_3Zn_{7.5-6.8}Ga_{3.5-4.2}$; τ_4 – $YbZn_{9.2-8.3}Ga_{1.8-2.7}$.

Table 5
Summarized data on interaction among the components in the Yb–M–Ga system.

IIIA	IVA	VA	VIA	VIIA	VIIIA			IB	IIB
Sc	Ti	V	Cr	Mn4	Fe3	Co13	Ni19	Cu10	Zn4
—	—	—	—	▲	△	△	△	△	△*
Y1	Zr	Nb	Mo	Tc	Ru	Rh3	Pd7	Ag9	Cd
△	—	—	—	—	2			▲	1
La	Hf	Ta	W	Re	Os	Ir3	Pt6	Au10	Hg
—	—	—	—	—	—			▲	—

▲ or △ – isothermal section built in the whole concentration region or in part of it, respectively; (N) – number of ternary compounds; — – no data available; * – this work.

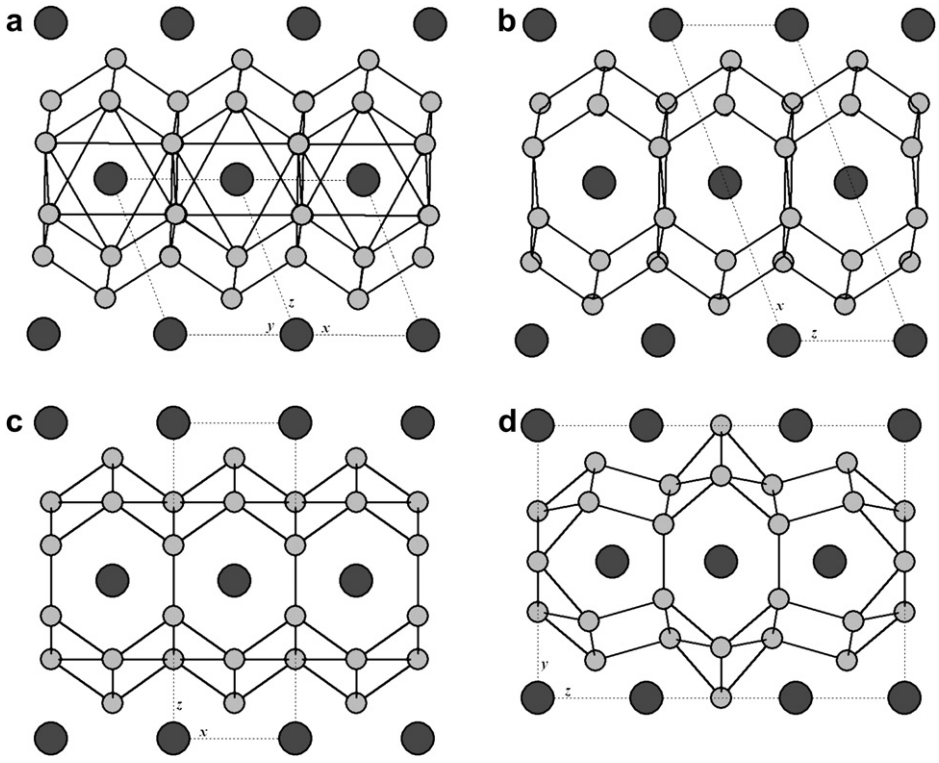

Fig. 12. Relations among $CaGa_4$ (a), $CaCu_{0.15}Ga_{3.85}$ (b), $BaAl_4$ (*c*) and La_3Al_{11} (d) structures. Dotted lines indicate the unit cell limits.

$YbZn_{0.25-0.5}Ga_{3.75-3.5}$ ($CaCu_{0.15}Ga_{3.85}$-type), $YbZn_{0.75-2}Ga_{3.25-2}$ ($BaAl_4$-type), $Yb_3Zn_{7.5-6.8}Ga_{3.5-4.2}$ (La_3Al_{11}-type) and $YbZn_{9.2-8.3}Ga_{1.8-2.7}$ ($BaHg_{11}$-type). An extended solid solution, based on the $YbZn_2$ compound, ranges up to the limit YbZnGa composition. The available data on the Yb–M–Ga systems points to the possibility of existence of new compounds and homogeneity ranges based on the partial substitution of the *d* atoms in the yet unexplored systems.

Acknowledgments

This work was partially supported by FCT, Portugal, under the contract No. PTDC/QUI/65369/2006. The FCT Grant No. SFRH/BPD/34840/2007 for the research work of Y.V. at ITN, Sacavém, Portugal is highly appreciated.

References

[1] Bodak OI, Gladyshevskii EI. Ternary systems containing rare earth metals. Lviv: Vyshcha Shkola, 1985 [in Russian].
[2] Grin Yu N, Gladyshevskii RE. Gallides. Moscow: Metallurgiya; 1989 [in Russian].
[3] Fedorchuk AO. Intermetallides of gallium and rare–earth elements. Synthesis, structure, properties. Thesis. 2006; Lviv [in Ukranian].
[4] Villars P, editor. Pearson's handbook, crystallographic data for intermetallic phases (desk ed.). OH: ASM Materials Park; 1997.
[5] Mason JT, Chiotti P. The ytterbium–zinc phase diagram. Trans AIME 1968;242:1167–71.
[6] Bruzzone G, Fornasini ML, Merlo F. Rare-earth intermediate phases with zinc. J Less Comm Met 1970;22:253–64.
[7] Palenzona A, Cirafici S. The ytterbium–gallium system. J Less Comm Met 1979;63:105–9.
[8] Yatsenko SP, Semyannikov AA, Semenov BG, Chuntonov KA. Phase diagrams of the rare earth metals with gallium. J Less Comm Met 1979;64:185–99.
[9] Cirafici S, Fornasini ML. Crystal structure of phases of the Yb–Ga system in the range 20–32 at.% Yb. J Less Comm Met 1990;163:331–8.
[10] Giedigkeit R, Niewa R, Schnelle W, Grin Yu, Kniep R. On the binary compound $YbGa_5$. Z Anorg Allg Chem 2002;628:1692–6.
[11] Massalski TB, editor. Ga–Yb (gallium–ytterbium), binary alloy phase diagrams. 2nd ed., 2. Ohio: ASM International, Materials Park; 1990. p. 1876–7.
[12] Pelleg J, Kimmel G, Dayan D. RGa_6 (R = rare earth atom), a common intermetallic compound of the R-Ga systems. J Less Comm Met 1981;81:33–44.
[13] Iandelli A. MX_2-Verbindungen der Erdalkali– und Seltenen Erdmetalle mit Gallium, Indium und Thallium. Z Anorg Allg Chem 1964;330:221–32.
[14] Heumann T, Predel B. Die Zustandsbilder von Gallium–Kadmium und Gallium–Zink. Z Metallkd 1958;49:90–5.
[15] Zivkovic D, Manasijevic D, Zivkovic Z. Thermodynamic study of Ga–Sn and Ga–Zn systems using quantitative differential thermal analysis. J Therm Anal Calorim 2003;74:85–96.
[16] Grin Yu, Hiebl K, Rogl P. Crystal structure and magnetism of YbT_xGa_{4-x}, T = Zn, Cd with the $BaAl_4$-type. J Alloys Compd 1995;227:L4–5.
[17] Nolze G, Kraus W. Powder cell for windows (version 2.3). Berlin: Federal Institute for Materials Research and Testing; 1999.
[18] Schwarzenbach D. Program LATCON. Switzerland: University of Lausanne; 1975.
[19] Rodriguez–Carvajal J, Roisnel T. FullProf.98 and WinPLOTR: new windows 95/NT applications for diffraction commission for powder diffraction, International Union for Crystallography, Newsletter №20 (May–August) Summer, 1998.
[20] Grin Yu, Ellner M, Predel B, Baumgartner B. Crystal structure of $CaCu_{0.15}Ga_{3.85}$– a new variant of the $BaAl_4$ structure type: structure analysis from X–ray powder diffraction data. J Solid State Chem 1995;114:342–5.
[21] Parthé E, Gelato L, Chabot B, Penzo M, Cenzual K, Gladyshevskii R. Typix, standardized data and crystal chemical characterization of inorganic structure types. Berlin: Springer–Verlag; 1994.
[22] Gumeniuk RV. Phase equilibria and crystal structure of compounds in the Ce–Ag–Ga, Tb–Ag–{Al, Ga} systems and some related. Thesis. 2003; Lviv [in Ukranian].